Princeton Plasma Physics Laboratory
NSTX Experimental Proposal

Title: HHFW Current Drive Experiments

OP-XP-312	**Revision:**	Effective Date: *(Ref. OP-AD-97)* Expiration Date: *(2 yrs. unless otherwise stipulated)*

PROPOSAL APPROVALS

Author: P. M. Ryan, J. R. Wilson, D. W. Swain, J. Hosea, T. K. Mau	Date 28 January 2003
ATI – ET Group Leader: G. Taylor	Date
RLM - Run Coordinator: S. M. Kaye	Date

Responsible Division: Experimental Research Operations

Chit Review Board (designated by Run Coordinator)

MINOR MODIFICATIONS (Approved by Experimental Research Operations)

NSTX EXPERIMENTAL PROPOSAL

HHFW Current Drive **XP 312**

1. Overview of planned experiment

Maintenance of plasma current by non-inductive means represents one of the most important mission elements of the NSTX Program and is of common interest to magnetic fusion energy sciences research. High power HHFW with an increased wavelength in the direction of the magnetic field via flexible control will be launched with a fast propagation velocity along the magnetic field line. This wave is expected to maximize momentum transfer to the electrons and drive plasma current non-inductively, while applying strong heating to increase plasma pressure and self-driven (bootstrap) current. The efficiency of combined HHFW-driven and self-driven current will be estimated by comparing global measurements in modest current plasmas with theory. An understanding of the underpinning physics of HHFW and self current drive and the techniques to ensure reliable operation at high power levels will contribute to future investigation of spherical torus plasmas sustained for longer durations in NSTX.

We propose to build upon the current drive results obtained in 2002 by operating the HHFW CD array at higher rf powers and higher electron temperatures. We intend to operate at time-invariant plasma conditions sufficiently long to unambiguously measure the effects of driven current by the external magnetics (reduced loop voltage). The time constant is expected to be on the order of 100 ms. The experiment aims to establish the current drive efficiency scaling with respect to density, electron temperature, and $k_{||}$. This information is needed for extrapolation to advanced integrated scenarios.

2. Theoretical/ empirical justification

Some of the experiment problems encountered last year will need to be eliminated prior to this experiment.

1. HHFW Power limitations
A voltage limit of ~13 kV (as measured at the feedpoint of the resonant loops) restricted operation to less than 3 MW for co-CD phasing and 1.5 MW for counter-CD phasing. It is believed that this was primarily due to arcing in the vacuum feedthroughs of the antenna straps. This has been addressed during the vessel opening and it is expected that we will be able to double the available power. The additional power will not only increase the driven current but will allow us to operate at higher (and more favorable) electron temperatures.

2. RF Noise pickup in the plasma control positioning coils.
RF noise pickup increased as the rf power increased and as the array phase angle decreased, to the point that plasma position control became difficult above about 2 MW. Increased shielding and filtering of the signal integrators are expected to alleviate this problem.

3. MHD activity during the rf application
MHD instabilities encountered when q(0) approached unity (and the concomitant central temperature collapses) were observed to reduce the non-inductive driven current. A low l_i, high

q(0) discharge with good MHD stability during the current flat-top is needed to measure the effects of HHFW CD on the loop voltage. Achievement of such a target plasma is the objective of XMP 027 and may be considered a prerequisite for this XP.

The absence of the Motional Stark Effect diagnostic prevented current density profiles from being measured during our CD experiments last year. However, the HHFW driven current can be estimated by establishing identical plasma conditions for co-CD and counter-CD phasing and assuming:

(1) Steady-state (t > L/R) conditions have been achieved.
(2) The plasma ohmic resistance is the same for both co- and counter-CD phasings.
(3) The HHFW driven current is proportional to the rf power.

Under these assumptions a 0D calculation of the driven current can be made from the measured loop voltage, after subtracting the calculated bootstrap current and compensating for the portion of the loop voltage that drives the changing magnetic stored energy.

Figure 1 shows a loop voltage comparison for $k_{||} = \pm 7.6\ \mathrm{m}^{-1}$, D_2 plasma, $B_T(0) = 0.445$ T; $I_p = 0.5$ MA. The HHFW power needed to obtain comparable core density and temperatures was 2.1 MW for co-CD and 1.1 MW for counter-CD; Thomson scattering measured $n_e(0) = 1.1\times10^{19}\ \mathrm{m}^{-3}$, $T_e(0) = 1.4$ keV. The 0.22 V difference in loop voltage for the two cases gives an estimated □I = 180 kA (110 kA co-CD, 70 kA counter-CD). However, the assumption of steady-state conditions is not well satisfied; internal MHD activity leads to a decrease in voltage difference with time.

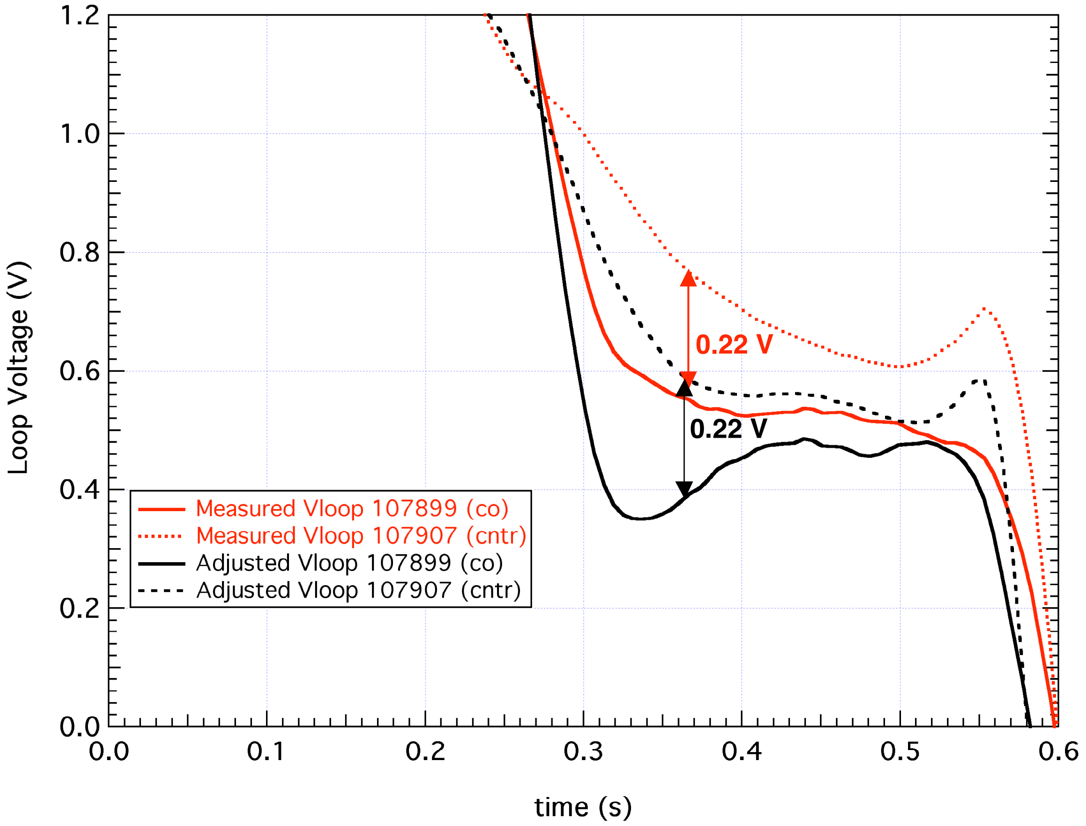

Fig. 1

HHFW current drive calculations have been made using the 2D full-wave code TORIC and the ray-tracing code CURRAY. The calculations are in general agreement with experimental estimates –

TORIC gives □I = 146 A (0.046 A/W) and CURRAY gives □I = 241 A (0.075 A/W). Both analyses indicate strong central power absorption, negligible damping on the H^+ minority, and a significant decrease in driven current due to trapped particle losses (30-40%).

Figure 2 shows the CD efficiency obtained last year in comparison with the fast wave current drive results from DIII-D and TFTR. One of the goals of this experiment is to obtain some data points at higher temperatures and to verify the density scaling.

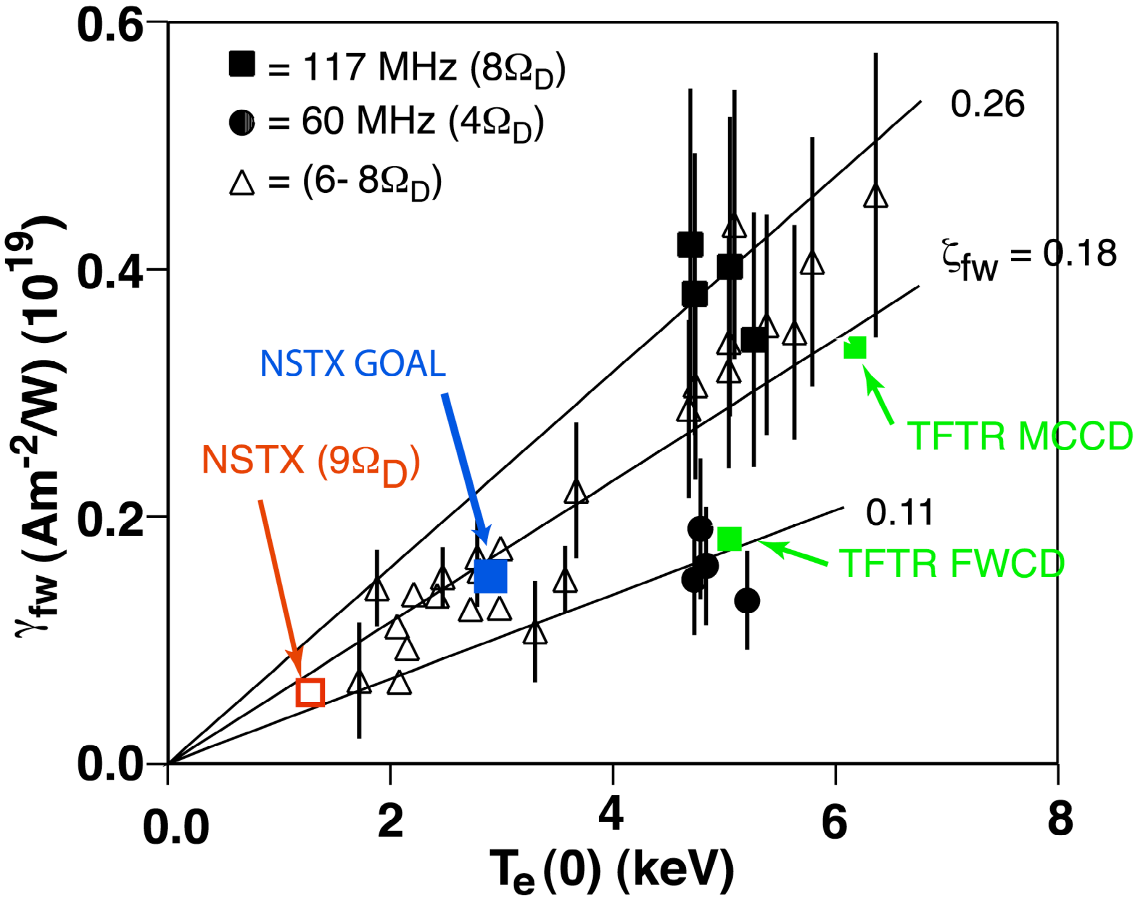

Fig. 2

T. K. Mau has calculated the current drive efficiency (I/P) as a function of Te based on shot 107899 (n_{e0} = 1.12×10^{19} m^{-3}, T_{e0} = 1.48 keV, T_i/T_e = 0.68). T_{e0} has been increased while keeping the temperature profile and the T_i/T_e ratio constant. The current drive efficiency for $k_{||}$ = 8 m^{-1} saturates around 2 keV while it continues to increase for $k_{||}$ = 3 m^{-1}. The wave velocity for $k_{||}$ = 8 m^{-1} corresponds to an 800 eV thermal velocity, while $k_{||}$ = 3 m^{-1} corresponds to a 4 keV thermal velocity. Simple theory predicts wave interactions with the electrons when the wave velocity is 0.5 to 2.0 times the thermal velocity, with higher efficiency corresponding to the higher wave velocity. However, the calculations also show more off-axis power deposition for the higher wave velocity, which cannot be explained by wave-particle velocity matching and depends on the ray trajectories for power propagation. This scaling will be checked by operation at two different values of $k_{||}$. Last year's operation at 3 m^{-1} gave higher CD efficiency (normalized to plasma density) than for 8 m^{-1} operation (0.043×10^{19} Am^{-2}/W as opposed to 0.034×10^{19}).

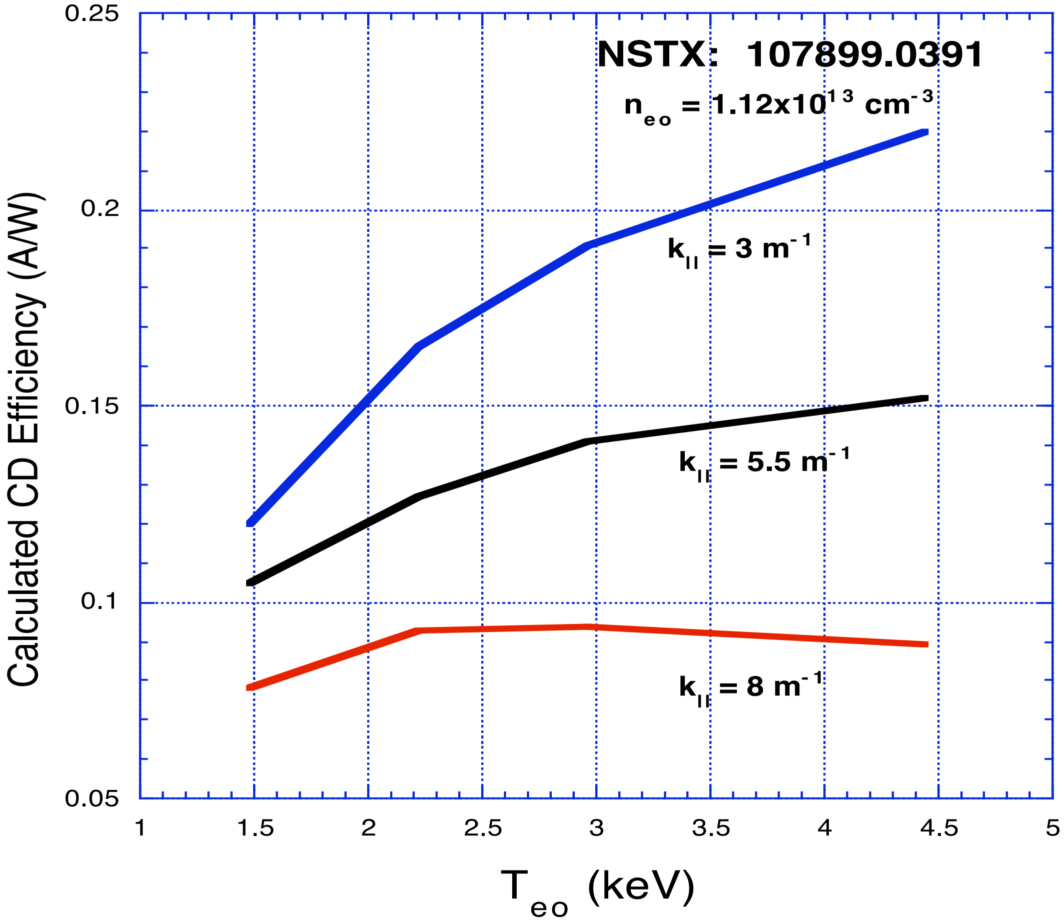

Fig. 3 CURRAY calculations of CD efficiency vs central electron temperature as a function of toroidal wave number.

3. Experimental run plan

The run plan is to scan rf power (linked to T_e) in both co-CD and counter-CD phases, for at least two densities and two values of $k_{||}$. Initial operation will be in He for better control of the density; later operation will be in D_2 for conditions more appropriate for advanced integrated scenarios.

Preliminary shots will be devoted to developing a quasi-steady state central electron temperature (150-200 ms) by raising the elongation or triangularity to delay the onset of MHD-driven temperature collapse associated with q(0) ~ 1. Shot 109765 will be used as the starting point. Early heating during the current ramp (50-110 ms) will be done with ~ 2 MW of rf power for reliability and repeatability. The 2-6 MW power scan will begin after current flattop is achieved (~110 ms). In the event of slow electron temperature rise that limits the pulse length of constant T_e, we will modulate the rf power (high power up to ~150 ms to increase heating rate, then decrease power to maintain T_e). If rf only is incapable of rapidly heating electrons and subsequently maintaining constant T_e, NBI injection will be employed (50 to 150 ms) for early heating and will overlap with the rf power for ~40 ms.

The first step will be to obtain current drive efficiency as a function of T_e (1.5-3 keV) for $k_{||} = 8$ m^{-1}. Start in low density plasma (n_{e0} ~ 1.5e19 m^{-3}) in order to maximize current drive efficiency, increase rf power (and presumably electron temperature) and compare co-CD and counter-CD loop voltages for the same central densities and temperatures. Locked mode signals and Z_{eff} will be monitored for lower density limits. For $k_{||} = 8$ m^{-1}, there is a large asymmetry in plasma loading and central heating efficiency for the two phasings. The maximum achievable power in counter-CD may be less than for co-CD, but the electron temperature may be the same due to better heating efficiency. The rf power may need to be modulated in time to maintain constant T_e, as mentioned above.

The second step will be to repeat the above for $k_{||} = 3$ m^{-1}. The current drive efficiency is expected to be better for $k_{||} = 3$ m^{-1} and $T > 1.5$ keV, but this high velocity wave may not heat cold electrons very effectively. For that reason we will first operate at ±60°, which has peaks of almost equal power at both 3 and 8 m^{-1}. The intent is to couple heating/CD power to the cold electrons at 8 m^{-1} and simultaneously drive current more efficiently by coupling to the heated electrons at 3 m^{-1}. CD efficiency comparisons will be made to pure 8 m^{-1} operation. After a successful temperature/power scan, one attempt will be made to shift from 60° to 30° operation during a shot (once constant temperature has been reached).

The third step will be to check density scaling by repeating a subset of either step 1 or step 2 shots (depending on which is more successful) for higher plasma density (n_{e0} ~ 3e19 m^{-3}).

The fourth step will be to repeat either step 1 or step 2 for D_2 plasmas.

Nominal plasma parameters: $I_p = 500$ kA, $B_T = 0.45$ T, t > 0.7 s, He, single-null diverted. Exact parameters will come from XMP 027 (shot 109765).

Shot list (42 good shots = two days operation):

1. Power scan at –90° ($k_{||} = 8$ m^{-1}, co-CD), low density ($n_{e0} = 1\text{-}1.5\times10^{19}$ m^{-3}), P = 2, 3, 4, 5, 6 MW (**5 shots**).
2. Power scan at +90° ($k_{||} = 8$ m^{-1}, counter-CD), low density ($n_{e0} = 1\text{-}1.5\times10^{19}$ m^{-3}), P = 2, 3, 4, 5, 6 MW (**5 shots**).
   Power and gas feed will be adjusted to give same T_{e0} and n_{e0}. Because of lower loading in counter-CD phasing, the voltage limit may be encountered at lower powers.
3. Power scan at –60° ($k_{||} = 3$ and 8 m^{-1}), low density ($n_{e0} = 1\text{-}1.5\times10^{19}$ m^{-3}), P = 2, 3, 4, 5, 6 MW (**5 shots**). Repeat one shot (power level TBD), switching from –60° to –30° when constant T_e is obtained (**1 shot**)

4. Repeat (3) for +60° phasing (**6 shots**).
5. Repeat steps 1-4 at high density ($n_{e0} = 3x10^{19}$ m^{-3}) for 3 and 5 MW (**8 shots**).
6. Repeat steps 1-4 at low density ($n_{e0} = 1$-$1.5x10^{19}$ m^{-3}) in D_2 for 2, 3.5, and 5 (**12 shot**s)

4. Required machine, NBI, RF, CHI and diagnostic capabilities

Machine will be operating at I_p ~ 500 kA, B_T ~ 0.45 T, He, for long (~ 1 s) pulses.

The RF system needs all six transmitters operating for long pulses at 600-750 kW each, phase control feedback, and I-V cube signals (phase and magnitude).

NBI (source A) should be prepared to operate if needed (80 kV, D, ~ 100 ms)

Need Thompson scattering system for T_e, n_e profiles, microwave reflectometer for edge density profiles, magnetics for EFIT equilibrium calculations, and Plasma TV for antenna hot spot surveillance. CHERS (for 1-2 shots), X-ray crystal desirable for T_i measurements, soft X-ray array and GEMS for temperature/power deposition informaion, and spectroscopy for Z_{eff} measurements (Z_{eff} profile would be desirable).

5. Planned analysis

EFIT analysis for internal inductance, surface voltage, and q-profile; TRANSP analysis for bootstrap current, parallel electric fields and driven current. Experimental measurements will be used to benchmark predictions of ray-tracing codes (CURRAY, HPRT, CQL3D) and full-wave codes (TORIC, AORSA).

6. Planned publication of results.

Preliminary results will be presented at the RF Power in Plasma conference (May, 2003).

PHYSICS OPERATIONS REQUEST

HHFW Current Drive **XP 312**

Machine conditions (specify ranges as appropriate)

I_{TF} (kG): **4.5** Flattop start/stop (s): **0/0.7**

I_P (MA): **0.5** Flattop start/stop (s): **0.11/0.6**

Configuration: **Lower Single Null/Double Null**

Outer gap (m): **0.05**, Inner gap (m): **0.05**

Elongation □: _____, Triangularity □: _____

□ and □ adjusted to keep q(0) > 1 for at least 400 ms.

Z position (m): **0.00**

Gas Species: **He**, Injector: **Midplane / Inner wall / Lower Dome**

NBI - Species: **D**, Sources: **A**, Voltage (kV): **80**, Duration (s): **0.1**

Early NBI heating to control q(0) is a contingency

ICRF – Power (MW): **2-6**, Phasing: **co-CD, cntr-CD** Duration (s): **0.5 s**

CHI: **Off**

Either: List previous shot numbers for setup: **109765 but with I_p = 500 kA**
Or: Sketch the desired time profiles, including inner and outer gaps, □, □, heating, fuelling, etc. as appropriate. Accurately label the sketch with times and values.

DIAGNOSTIC CHECKLIST

HHFW Current Drive **XP 312**

Diagnostic system	**Need**	**Desire**	**Requirements** (timing, view, etc.)
Magnetics	✓		
Fast visible camera			
VIPS-1			
VIPS-2			
SPRED			
GRITS			
Visible filterscopes	✓		
VB detector	✓		
Midplane bolometer			
Diamagnetic flux			
Density interferometer (1mm)			
FIReTIP interf'r/polarimeter		✓	
Thomson scattering	✓		
CHERS			
NPA		✓	
X-ray crystal spectrometer			
X-ray PHA			
EBW radiometer			
Mirnov arrays	✓		
Locked-mode detectors	✓		
USXR arrays	✓		
2-D x-ray detector (GEM)		✓	
X-ray tangential camera			
Reflectometer (4 ch.)			
Neutron detectors			
Neutron fluctuations			
Fast ion loss probe			
Reciprocating edge probe			
Tile Langmuir probes			
Edge fluctuation imaging			
H-alpha cameras (1-D)		✓	
Divertor camera (2-D)			
Divertor bolometer (4 ch.)			
IR cameras (2)			
Tile thermocouples			
SOL reflectometer	✓		